

LASER COOLING

DOI: 10.1070/QEL16138

Multiparticle losses in a linear quadrupole Paul trap

I.A. Semerikov, I.V. Zalivako, T.V. Shpakovskii, A.S. Borisenko, K.Yu. Khabarova, V.N. Sorokin, N.N. Kolachevsky

Abstract. **A linear quadrupole Paul trap is fabricated for capturing magnesium and aluminium ions. An experimental cycle performed has demonstrated ion capture and holding in a trap with an average ion lifetime of 1.7 s. Modelling of ion dynamics in the trap shows that the main mechanism responsible for losses of hot ions is multiparticle interaction, which results in that a kinetic energy of some ions increases and they leave the trapping zone. This mechanism is completely suppressed if ions are cooled. Another mechanism is the charge exchange; however, it is not substantial at a high average energy of ions produced in the result of an electron impact. Parameters of the trap allow one to perform precision spectroscopic measurements and to control ion quantum states.**

Keywords: *quadrupole Paul trap, multiparticle losses, electron impact.*

1. Introduction

In many physical problems such as time and frequency metrology, precision spectroscopy, quantum calculations and simulation it is necessary to isolate an atom or an ion from ambient fields and minimise its average kinetic energy. The presence of an ion charge makes it possible to capture it in a Paul trap with combined constant and radio-frequency (RF) electric fields [1]. In such a trap, both single ions and ensembles can be captured; by means of laser cooling one can reach temperatures corresponding to the lowest vibrational states of a trap potential [2, 3]. Low ion temperatures, long lifetimes in the trap, and actually total insulation from external action make it possible to investigate spectrally narrow transitions in ions and employ them for solving a wide range of fundamental and applied problems [4–6].

The ion lifetime in a trap is determined by a number of factors: a charge exchange with molecules of a residual gas in a chamber, a phase shift between RF potentials applied to trap electrodes, parasitic charges and contact potential on trap electrodes and other mechanisms, which increase the kinetic energy of ions [7–9]. While trapping an ion ensemble, a substantial mechanism affecting the lifetime is the Coulomb interaction between ions, which is responsible for additional frequencies arising in the spectrum of motion.

Ions are loaded to a trap by the method of electron impact [10]: neutral atoms are ionised by the electron beam directly in the capturing zone. In this case, the energy of trapped ions can be of the order of the trap potential well depth, which is conventionally up to 10 eV. In the latter case, the Coulomb repulsion will lead to losses reducing the lifetime and limiting the maximal number of trapped particles.

Since we plan to employ the trap described in the present work for precision spectroscopy of clock transition in aluminium ion [4] and for quantum state manipulation, the ion lifetime in the trap should not restrict the experimental cycle duration. The desirable lifetime should be at least an hour, which provides the measurement cycle with sufficient statistics. It is known that the lifetime of an ion in cryogenic traps can reach several months due to the extremely low pressure of residual gases [11]; however, at room temperature this time becomes shorter. In the present work, we experimentally and theoretically study the mechanism of multiparticle losses in a linear RF Paul trap, developed for trapping $^{27}Al^+$ and $^{24}Mg^+$ ions and show that the trap can be used for solving the problems stated.

2. Experimental setup

The ion trap developed refers to linear quadrupole Paul traps (Fig. 1). It comprises four cylindrical electrodes, from which two are grounded and the other two are connected to a potential of type $U_{dc} + V_{ac}\cos\omega t$. Here, U_{dc} is a constant potential component, ω is the frequency of alternating field, and V_{ac} is the amplitude of potential oscillation. The frequency ω may vary within the range of 5–20 MHz. A quadrupole potential produced by the electrodes restricts ion movement in the

I.A. Semerikov, T.V. Shpakovskii P.N. Lebedev Physics Institute, Russian Academy of Sciences, Leninsky prosp. 53, 119991 Moscow, Russia; Russian Quantum Centre, ul. Novaya 100, Skolkovo, 143025 Moscow, Russia; e-mail: ilia179@mail.ru;
I.V. Zalivako, A.S. Borisenko P.N. Lebedev Physics Institute, Russian Academy of Sciences, Leninsky prosp. 53, 119991 Moscow, Russia; Russian Quantum Centre, ul. Novaya 100, Skolkovo, 143025 Moscow, Russia; Moscow Institute of Physics and Technology (State University), Institutskii per. 9, 141707 Dolgoprudnyi, Moscow region, Russia; e-mail: zalivako.ilya@yandex.ru;
K.Yu. Khabarova, N.N. Kolachevsky P.N. Lebedev Physics Institute, Russian Academy of Sciences, Leninsky prosp. 53, 119991 Moscow, Russia; Russian Quantum Centre, ul. Novaya 100, Skolkovo, 143025 Moscow, Russia; Federal State Unitary Enterprise 'All-Russian Scientific-Research Institute of Physical-Technical and Radiotechnical Measurements', 141570 Mendeleevo, Moscow region, Russia; e-mail: kseniakhabarova@gmail.com, kolik@lebedev.ru;
V.N. Sorokin P.N. Lebedev Physics Institute, Russian Academy of Sciences, Leninsky prosp. 53, 119991 Moscow, Russia; e-mail: sovn@sci.lebedev.ru

Received 17 May 2016, revised 12 July 2016
Kvantovaya Elektronika **46** (10) 935–940 (2016)
Translated by N.A. Raspopov

radial direction. The electrodes have a length of l = 74 mm and radius of r = 1 mm. A large electrode length reduces the influence of edge effects on the field linearity at a trap centre. A distance from the electrode surface to the trap centre is r_0 = 1.475 mm. The ratio r_0/r is close to the optimal value of 1.1468, at which the potential produced by cylindrical electrodes is the most close to quadrupole. Deviation from the optimal value is explained by necessity of convenient optical access. Near the trap centre, deviation of the potential from an ideal quadrupole is characterised by a geometrical factor $\varkappa$. 2D calculation with the COMSOL Multiphysics software has shown that in our trap $\varkappa = 0.98 \pm 0.01$, which is close to the optimal value. The electrodes are fabricated from tungsten to minimise the heating of ions in the trap due to thermal fluctuations of defects in the crystal lattice of electrodes and to the corresponding fluctuations of the electric field in the trap [12].

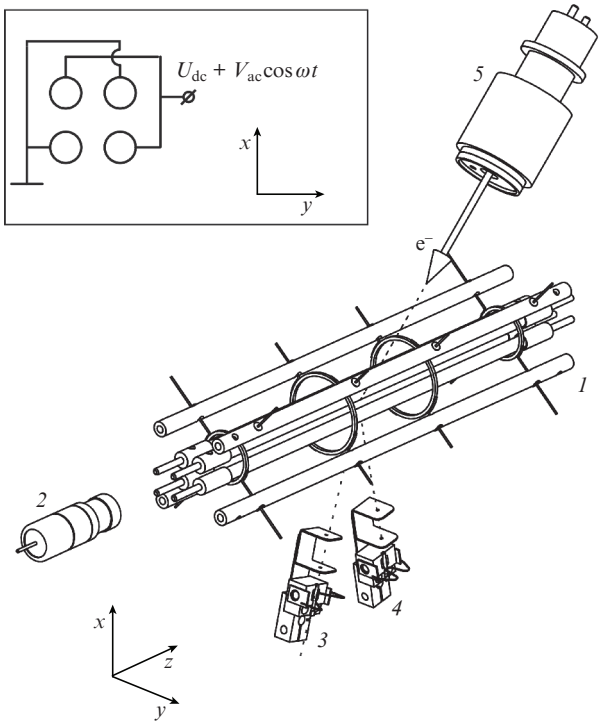

Figure 1. Schematic of the setup for capturing and detecting ions in a trap (not to scale): (*1*) linear quadrupole Paul trap; (*2*) channel electron multiplier (CEM); (*3*) and (*4*) sources of neutral aluminium and magnesium atoms, respectively; (*5*) electron gun. The inset shows the electric circuit of electrode connections.

In the axial direction ions are kept by four ring electrodes to which a constant positive potential is applied. The rings that are closer to the trap centre have a diameter of 12.5 mm; the diameter of the other two rings is 8 mm. A distance between two internal rings is 18.5 mm and between the external rings it is 63.5 mm. Potentials of each of the ring electrodes can be varied independently.

Rods that produce the capturing field in the trap are surrounded by additional four cylindrical electrodes, which are used for compensating parasitic static electric fields at a centre of the trap and minimising micromotions caused by these fields. Potentials of these additional rods can also be varied independently.

A high-frequency voltage of high amplitude applied across the trap electrodes (several hundred volts) is produced by a resonant transformer (Fig. 2). A secondary coil of the transformer is wound by litzendraht wire on a fluoroplastic base and has the inductance of $L \approx 3.5$ μH. This coil and the RF electrodes having a capacitance of approximately 20 pF form a resonant circuit with a resonant frequency of about 18.2 MHz. The primary coil is a single turn of wire inside the secondary coil. The generator and load are matched in impedance by varying the mutual induction factor between the primary and secondary coils, which is realised by tuning the angle between their axes. The transformer resonant frequency is tuned by using a capacitor connected in parallel to the trap. An amplified signal from an oscillator feeds the resonant transformer (Fig. 2).

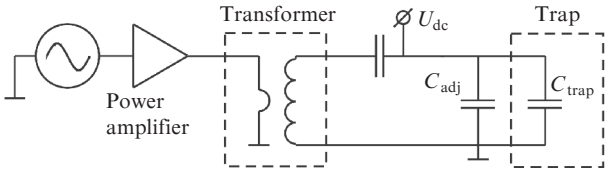

Figure 2. Connecting the resonant transformer: C_{adj} is the capacitor for adjusting the frequency of the resonant circuit; C_{trap} is the capacitance of trap electrodes.

Ions in the trapping zone are produced in the process of impact ionisation of neutral atoms by the electron beam. Atom guns are the sources of neutral Al and Mg atoms. Those are tantalum tubes of diameter 0.8 mm filled with aluminium or magnesium chip. Tantalum was chosen due to its low chemical activity and high melting temperature. A small tube dimension reduces the temperature lag effect of atomic sources. The oxide film arising on a metal surface is destroyed by the flux added to metal chips. Heating is performed by the electric current flowing through a tantalum wire wound on the tubes. Outgoing atoms flying through a diaphragm produce a collimated beam with a divergence angle of about 10°, which crosses the centre of the trap. The electron beam is generated by an EGA-1012 electron gun (Kimpball Physics). The energy of electrons can be varied in the range 5–1000 eV. The trap also captures ionised atoms of the background gas.

Ions are detected by the channel electron multiplier (CEM) used in a single-ion counting regime, which is placed at the trap axis (see Fig. 1). The signal from the SEM passes to a pulse counter with a time resolution of 5 ns.

A getter-ion pump maintains vacuum at a pressure of less than 10^{-10} mbar at switched-off atom sources and electron gun.

3. Trapping ions and determining ion lifetime in the trap

The character of the ion motion in a linear Paul trap is determined by the two dimensionless parameters:

$$a = \frac{4QU_{dc}}{m\omega^2 r_0^2}, \quad q = \frac{2QV_{ac}}{m\omega^2 r_0^2}, \tag{1}$$

where Q is the ion charge and m is its mass. If parameters a and q fit the stability range (Fig. 3), then an ion is captured in a trap [13]. In our experiment the trap operated at a frequency of $\omega = 2\pi \times 5.134$ MHz at a voltage amplitude across electrodes $V_{ac} = 130$ V and constant potential component $U_{dc} = 0$, which corresponds to the parameters $a = 0$ and $q = 11.08/m_0$, where m_0 is the molecular mass of the ion in atomic units (for singly charged ions). The depth of the trap can be estimated by the formula

$$U_{dep} \approx \frac{Q^2 V_{ac}^2}{4m\omega^2 r_0^2}, \qquad (2)$$

which at the parameters given above yields $U_{dep} \approx 180/m_0$, where U_{dep} is taken in electron-volts.

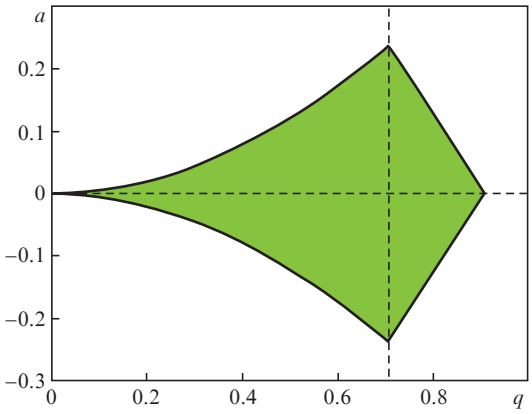

Figure 3. Stability diagram for the ion in a RF trap. The filled domain of parameters corresponds to stable capturing of ions in the trap.

From the stability diagram one can see that the parameter a along with the constant voltage component on rod electrodes U_{dc} may vary in mostly wide ranges keeping stability of ion motion if $q \approx 0.7$. In this case, the trap becomes least sensitive to external electric fields.

Efficiency of ion trapping was verified by investigating the dependence of the number of trapped particles on the duration of trap loading. For loading ions, an electron gun with the electron energy of 500 eV and emission current of 5 μA is switched on. At a lower energy, electrons emitted by the gun strongly deviate under the action of the trap field and do not reach the centre.

Experiment started at the RF field switched on and at the potential across the ring electrodes $V_{axial} = 1000$ V. In a time interval of the trap loading t_{load}, which in the experiment varied from 0.1 to 10 s, the electron beam is cut off. Trapped ions are stored in the trap for time $t_s = 0.1$ s in order to let the untrapped ions leave the trapping zone. Then the two ring electrodes closest to the CEM were grounded by a fast switch and ions were pushed out towards a detector by the field of another pair of ring electrodes. A counter with a detection time window of 1 ms connected to the CEM started operation synchronously with the grounding of the ring electrodes. The voltage on the CEM was 2 kV, the discrimination level of the counter chosen for maximising the signal-to-noise ratio was equal to –5 mV; the pressure in a chamber was $\sim 10^{-9}$ mbar.

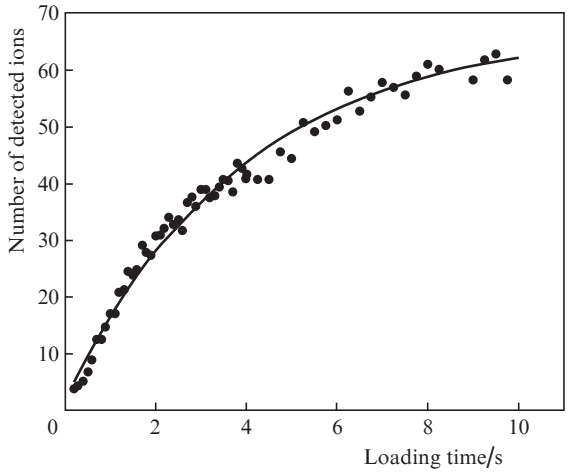

Figure 4. Dependence of the number of detected particles on the trap loading time t_{load}.

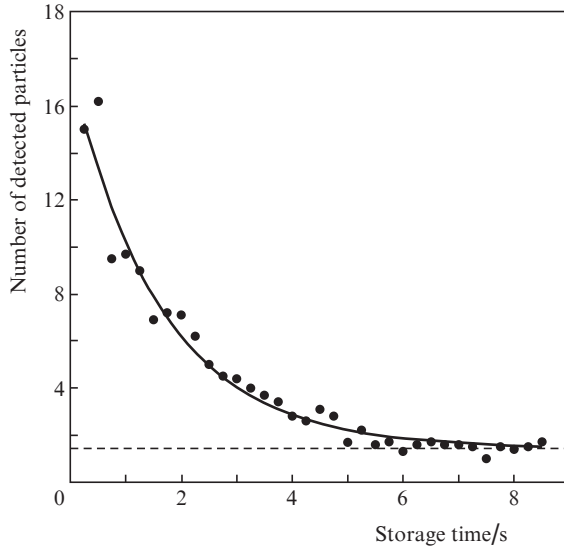

Figure 5. Number of detected particles vs. storage time t_s. The solid curve is exponential approximation of data.

The dependence of the number of detected ions on the trap loading time t_{load} at the storage time $t_s = 0.1$ s is presented in Fig. 4. The characteristic time of ion loading to the trap is 3.9 s. Then the efficiency of ion loading to the trap falls, which, probably, is related to a higher ion loss rate from the trap due to their mutual interaction.

The ion lifetime in the trap was determined from the dependence of the number of detected ions on the storage time t_s at a constant loading time $t_{load} = 1$ s. At such t_{load}, the number of ions captured in the trap is sufficient for providing the necessary signal-to-noise ratio. Measurement results are given in Fig. 5.

The measured ion lifetime in the trap τ_{life} is 1.7 s, which is much longer than the characteristic time needed for Doppler cooling (about 1 ms) [14]. However, in experiments with single ions (precision spectroscopy, single-particle quantum state manipulation) this time is not sufficient and the mechanisms limiting the ion lifetime in the trap should be studied.

4. Numerical simulation of ion dynamics in the trap

For explaining the experimentally observed rate of ion departure from the trap, we have theoretically studied possible mechanisms of ion losses. As discussed in Introduction, there are two main mechanisms of trap losses: interaction between ions and ion collisions with a neutral background gas, which results in the charge exchange. Influence of the first mechanism was estimated by simulating numerically the dynamics of high-energy ions in a trap field. The second mechanism has also been estimated.

Assuming that the trap potential along x and y axes is ideally quadrupole and along z axis it is harmonic, one can write out the equations of particle motion taking into account the Coulomb interaction of ions:

$$\frac{\mathrm{d}^2 x_k}{\mathrm{d}t'^2} + 2q\cos(2t')x_k = \frac{Q^2}{\pi\varepsilon_0\omega^2 m}\sum_{i=1,i\neq k}^{N}\frac{x_k - x_i}{r_{ik}^{3/2}}, \tag{3}$$

$$\frac{\mathrm{d}^2 y_k}{\mathrm{d}t'^2} - 2q\cos(2t')y_k = \frac{Q^2}{\pi\varepsilon_0\omega^2 m}\sum_{i=1,i\neq k}^{N}\frac{y_k - y_i}{r_{ik}^{3/2}}, \tag{4}$$

$$\frac{\mathrm{d}^2 z_k}{\mathrm{d}t'^2} + \frac{4\omega_z^2}{\omega^2}z_k = \frac{Q^2}{\pi\varepsilon_0\omega^2 m}\sum_{i=1,i\neq k}^{N}\frac{z_k - z_i}{r_{ik}^{3/2}}, \tag{5}$$

where x_k, y_k, z_k are coordinates of the kth ion; r_{ik} is the distance between ith and kth ions; t' is the dimensionless time parameter such that $t' = \omega t/2$; t is the time; ε_0 is the permittivity of free space; and ω_z is the oscillation frequency along the z axis. Here, the left-hand side of the equations describes the ion interaction with the RF field, and the right-hand side is responsible for the interaction between the ions.

In modelling, the following parameters close to experimental trap parameters have been chosen: $q = 0.4$, $\omega = 2\pi \times 5.134$ MHz, $\omega_z = 100$ s^{-1}, the ion mass and charge corresponded to a singly ionised magnesium ion ($m_0 = 25$ amu). The calculation included a cylindrical domain with a radius $r = 1$ mm and length $l = 10$ mm, which approximately corresponded to the dimensions of our trap.

Initial conditions were chosen as random coordinates with a uniform distribution inside the calculation domain. Initial velocities of particles satisfied the Maxwellian distribution at a temperature of 1000 K. Particles crossing the domain boundary were assumed lost and excluded from further calculations. Several calculations were performed at various realisations of initial conditions. Initially, calculations included 30 particles; however, in first 10 ms the most of them were lost. These particles were considered not trapped and were excluded from calculations. They could not be detected in experiments.

In Fig. 6, an average particle kinetic energy vs. the storage time is shown. One can see that the average energy falls stepwise, which occurs at instants when a particle (or particles) leaves the trap. This effect is similar to evaporation cooling [15]: ions, due to collisions with each other, exchange energy, and when an ion acquires an energy sufficient for leaving the trap, it is released; the temperature of the rest gas falls. One can also see that in time intervals between particle departures the average kinetic energy of the ion does not change.

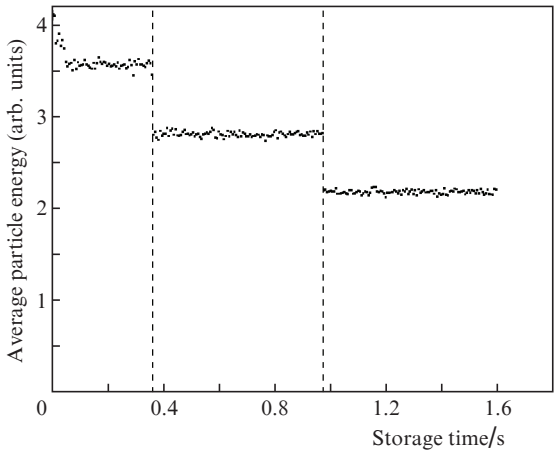

Figure 6. Average kinetic energy of ions in the trap vs. the storage time (simulation). The stepwise decreases in energy at instants ~0.4 and ~1 s are related to the escapes of particles from the trapping zone.

The simulated dependence of the number of particles in the trap on the storage time is presented in Fig. 7. If the initial temperature of particles captured in the trap is reduced, the rate of ion losses substantially falls. This is related to the fact that the value of energy fluctuations of a single ion needed to leave the trap increases, whereas the probability of this event reduces. The rate of the particle loss observed from calculations is about 3 s^{-1} for eight initial particles, which corresponds to experimental values (see Fig. 5). Since losses related to this mechanism reduce as the ion temperature falls, we expect that the lifetime will substantially increase after laser cooling. Note also that at a lower number of particles the rate of losses reduces and attains zero for a single ion. Thus, the mechanism considered would not hinder further experiments in which we plan to study strongly cooled single ions.

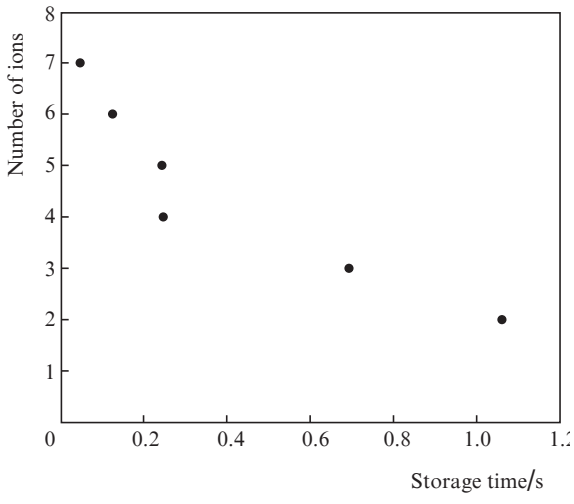

Figure 7. Number of ions in the trap vs. storage time (numerical simulation).

The charge exchange in collisions between trapped ions and neutral atoms of the buffer gas may also lead to losses. At the trap parameters corresponding to experimental conditions, the trap is stable only for ions with mass $m_0 > 12$ amu in the case of single ionisation. Hence, if a captured ion gives away its charge in collisions with an atom of mass $m_0 < 12$ amu, then the new ion will no more be captured in the trap and will leave it as well.

For estimating the maximal rate of losses, we assume that the charge exchange between the trapped ion and atom of the buffer gas results in a loss of the ion. Then the average lifetime of a single ion is

$$\tau_{ex} = \frac{1}{\langle v_{rel} \rangle n_{buf} \sigma_{ex}}, \quad (6)$$

where $\langle v_{rel} \rangle$ is the average velocity of ion motion relative to neutral particles; n_{buf} is the concentration of neutral particles of the background gas near the trap; and σ_{ex} is the non-resonant charge exchange cross section. The number of ions in the trap N depends on time as $N = N_0 \exp(-t/\tau_{ex})$.

For finding the concentration of neutral particles at the trap centre, we have used results of experiments on the efficiency of trap loading. A straight line approximated an initial part of the dependence of the number of ions on the time of loading. We neglected losses of ions in the trap; it was assumed that all atoms ionised in a trap volume are captured. Then the number of ionisation events in a trap volume per unit time equals the inclination of the straight line $k_{ion} = 12\ s^{-1}$. On the other hand,

$$k_{ion} = \frac{n_{buf} I_{gun} V_{trap} \sigma_{ion}}{e S_{gun}},$$

where $I_{gun} = 10^{-5}$ A is the emission current of the electron gun; $V_{trap} = 2 \times 10^{-8}\ m^3$ is the trapping zone volume; $\sigma_{ion} \approx 10^{-20}\ m^2$ is the ionisation cross section [10]; and $S_{gun} = 7 \times 10^{-5}\ m^2$ is the cross-sectional area of the electron gun beam at the trap input. From this formula one obtains an estimate of the buffer gas concentration in the trapping zone: $n_{buf} \approx 10^{12}\ m^{-3}$. This estimate approximately coincides with data from a vacuum sensor in the ion pump.

Since the ion velocity in the trap v_{ion} is well above the thermal velocity of buffer gas particles, the relative velocity is mainly determined by ion motion: $\langle v_{rel} \rangle \approx \langle v_{ion} \rangle$. At these parameters the average velocity of particles in the trap, obtained from numerical simulation, was $10^4\ m\ s^{-1}$. The cross section of the non-resonant charge exchange σ_{ex} is determined by particle geometrical dimensions and is equal to $\sim 10^{-20}\ m^2$ [16].

The lifetime τ_{ex} calculated by formula (6) and determined by the charge exchange is $\sim 10^4$ s, which is much greater than experimentally observed values. From this estimate follows that exchange mechanism of ion losses can be neglected in the case of a large average kinetic energy of trapped particles.

Thus, the main mechanism of ion losses in our trap is multiparticle interaction. In the considered case of a high average particle energy the described mechanism is the main factor that limits the ion lifetime in the trap. It is substantially suppressed at lower ion velocities, which can be realised with laser cooling or by employing sympathetic cooling [17].

5. Conclusions

We have designed a linear RF Paul trap, and ion trapping and holding have been demonstrated. Ions were produced by an electron impact, which provides their high initial energies in the trap that are comparable to the trap depth. The characteristic ion lifetime in the trap measured by the CEM, which detected the ion departure, was 1.7 s.

The mechanism of ion losses was studied by simulating numerically the dynamics of hot ions in the trap taking into account multiparticle interaction. It was shown that in the case of high kinetic energies of trapped particles (corresponding to a temperature of 10000 K) the main mechanism is the ion–ion interaction, whereas the charge exchange mechanism of losses can be neglected. In the result of modelling it was established that the rate of multiparticle losses rapidly falls under reducing the temperature of the ion cloud and the number of ions. It is concluded that this mechanism would not limit the ion lifetime in the case of laser cooling. Thus, there are possibilities for performing planned experiments on precision spectroscopy of aluminium ions at the wavelength of 267 nm and for manipulating quantum states in aluminium and magnesium ions.

Further we plan to carry out experiments on laser Doppler cooling of magnesium ions at the resonance wavelength of 280 nm [18]. Our estimates show that after a cooling cycle the ion lifetime may reach dozens of minutes, which will make it possible to study ion crystals and dynamics of sympathetic cooling in the case of aluminium ions. In addition, laser spectroscopy will uniquely identify the type of ions, in contrast to the non-selective CEM detection method.

Acknowledgements. The work was supported by the Russian Science Foundation (Project No. 16-12-00096).

References

1. Paul W., Raether M. *Z. Phys.*, **140**, 262 (1955).
2. Wineland D.J., Dehmelt H. *Bull. Am. Phys. Soc.*, **20**, 637 (1975).
3. Monroe C., Meekhof D.M., King B.E., Jefferts S.R., Itano W.M., Wineland D.J., Gould P. *Phys. Rev. Lett.*, **75** (22), 4011 (1995).
4. Rosenband T., Hume D.B., Schmidt P.O., Chou C.W., Brusch A., Lorini L., Oskay W.H., Drullinger R.E., Fortier T.M., Stalnaker J.E., Diddams S.A., Swann W.C., Newbury N.R., Itano W.M., Wineland D.J., Bergquist J.C. *Science*, **319** (5871), 1808 (2008).
5. Steane A. *Appl. Phys. B*, **64**, 623 (1997).
6. Cirac J.I., Zoller P. *Phys. Rev. Lett.*, **74** (20), 4091 (1995).
7. Harmon T.J., Moazzan-Ahmadi N., Thompson R.I. *Phys. Rev. A*, **67**, 013415 (2003).
8. Berkeland D.J., Miller J.D., Bergquist J.C., Itano W.M., Wineland D.J. *J. Appl. Phys.*, **83** (10), 5025 (1998).
9. Andelkovic Z., Cazan R., Nörtershäuser W., Bharadia S., Segal D.M., Thompson R.C., Jöhren R., Vollbrecht J., Hannen V., Vogel M. *Phys. Rev. A*, **87**, 033423 (2013).
10. Boivin R.F., Srivastava S.K. *J. Phys. B*, **31** (10), 2381 (1998).
11. Oskay W.H., Diddams S.A., Donley E.A., Fortier T.M., Heavner T.P., Hollberg L., Itano W.M., Jefferts S.R., Delaney M.J., Kim K., Levi F., Parker T.E., Bergquist J.C. *Phys. Rev. Lett.*, **97** (2), 020801 (2006).
12. Herrmann M. *Dissertation an der Fakultät der Physik der Ludwig–Maximilians–Universität* (München, 2008).
13. Leibfried D., Blatt R., Monroe C., Wineland D. *Rev. Mod. Phys.*, **75**, 281 (2003).
14. Rosenband T., Schmidt P.O., Hume D.B., Itano W.M., Fortier T.M., Stalnaker J.E., Wineland D.J. *Phys. Rev. Lett.*, **98** (22), 220801 (2007).

15. Petrich W., Anderson M.H., Ensher J.R., Cornell E.A. *Phys. Rev. Lett*., **74** (17), 3352 (1995).
16. Rapp D., Francis W.E. *J. Chem. Phys*., **37**, 2631 (1962).
17. Kielpinski D., King B.E., Myatt C.J., Sackett C.A., Turchette Q.A., Itano W.M., Monroe C., Wineland D.J., Zurek W.H. *Phys. Rev. A*, **61** (3), 032310 (2000).
18. Hemmerling B., Gebert F., Wan Y., Nigg D., Sherstov I.V., Schmidt P.O. *Appl. Phys. B*, **104** (3), 583 (2011).